Journal of
Water & Climate Change

IWA PUBLISHING

Journal of Water and Climate Change Vol 15 No 3, 1018 doi: 10.2166/wcc.2024.440

Spatiotemporal analysis of precipitation variability based on entropy over Iran

Mohammad Darand [a,b,*] and Farshad Pazhoh[a]

[a] Department of Climatology, University of Kurdistan, Sanandaj, Iran
[b] Department of Zrebar Lake Environmental Research, Kurdistan Studies Institute, University of Kurdistan, Sanandaj, Iran
*Corresponding author. E-mail: m.darand@uok.ac.ir

MD, 0000-0001-9254-1370

ABSTRACT

This study was conducted to identify variability in precipitation entropy and specify the water resource zones of Iran. Precipitation data with a spatial resolution of 0.25° during the period from 01/01/1962 to 31/12/2019 were used. For the investigation of variability in precipitation entropy over Iran, two indices were applied: entropy and disorder. The results demonstrated that the maximum occurred at the Caspian coasts and the minimum observed at the southern coasts of Iran. Most areas over the country have encountered negative trends in the entropy index. The rates of the entropy index have decreased, and the mean rate of the disorder index has increased. An analysis of variability in the extension of water resource zones in terms of the entropy index demonstrated that Iran could be divided into four zones: abundant and permanent; deficient and permanent; deficient and concentrate; and abundant and concentrate. After 1998, the abundant, permanent zone in the northern, high-altitude half of the country, the abundant, concentrated zone in the southwest, and the zone with deficient and permanent precipitation in the northern half of the central parts have become less extensive, while the zone with deficient and concentrate precipitation has become more extensive toward the northern latitudes.

Key words: concentration, entropy, Iran, precipitation, variability, water area

HIGHLIGHTS

- This study was conducted to identify variability in precipitation entropy and specify the water resource zones of Iran.
- The maximum values of the entropy index occurred at the Caspian coasts and the minimum was observed at the southern coasts of Iran.
- The mean entropy index over Iran has gradually decreased since 1998.
- The deficient and concentrate precipitation zone has become more extensive toward the northern latitudes.

GRAPHICAL ABSTRACT

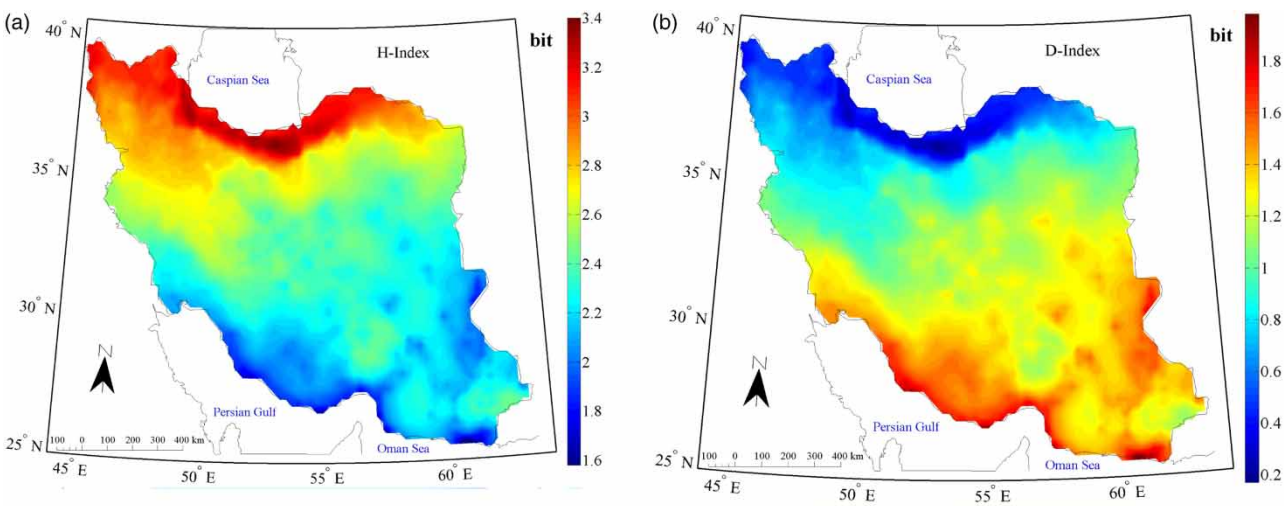

1. INTRODUCTION

Precipitation is one of the most variable climatic elements, exhibiting plenty of temporal and spatial variations. There is significant variation in precipitation, especially in regions with lower amounts. With a mean annual precipitation of about 250 mm, Iran is considered an arid country, as the global average is 960 mm. Although Iranians have long adapted to low precipitation and its fluctuations, any change in the amount or distribution of precipitation will transform life in the country (Masoudian 2011). Precipitation, as a climatic element and process, is highly sensitive to climatic changes. Any fundamental change in the amount, type, and pattern of precipitation can have significant consequences (Tegart *et al.* 1990), affecting other elements of climate as well as biological, economic, and social activities in a feedback loop. Therefore, it is of great importance to understand variability in precipitation due to its significance in a large number of areas, including natural areas (as in the hydrologic cycle or the general circulation of the atmosphere) and economic areas (as in agriculture, industry, or services) (Marengo *et al.* 2001). In this research, the *H*-Index and the *D*-Index are used to identify spatiotemporal changes in precipitation and analyze water resources over Iran. Applying the theory of entropy in studies can contribute to better analysis and understanding of the variability in the spatial patterns of the phenomena being analyzed (Silva *et al.* 2017).

Masoudian (2006) analyzed the water resource regions over Iran using the index of precipitation entropy from 1951 to 1999 and statistical analysis methods for data analysis. Also, the index measures the uncertainty in the annual share of precipitation. The research results demonstrated that the *H*-Index could express the characteristics of precipitation in the country. The *H*-Index was combined with the annual precipitation of Iran to enable the zoning of the country in terms of the potential availability of water resources, and it was found that there were four water resource availability regions in Iran. Zamani *et al.* (2018) investigated the daily, seasonal, and annual behavior of precipitation concentration in Jharkhand State on the Indian Peninsula. According to their results, plenty of irregularity and inconsistency was observed in different parts of the region due to heavy daily precipitation. Simultaneously, there was an incremental trend in annual precipitation in the east and northeast, which reduced values for the precipitation concentration index. Unlike during the peak precipitation season (summer), there was an incremental trend in winter for precipitation concentration. Roushangar & Alizadeh (2018) investigated annual precipitation change detection in Iran using the function decomposition method. According to their results, precipitation entropy decreased as latitude dropped in the south, exhibiting a decreasing trend. They also found a close relationship between longitude and mean annual entropy in Iran. In his analysis of the trend and homogeneity of precipitation in Iran, Javari (2016) stated that there was great diversity in seasonal precipitation patterns in Iran, and less spatial coherence was observed concerning the temporal patterns in seasonal precipitation. He also suggested that the variation in seasonal precipitation exhibited a decreasing trend in the central and eastern regions and an incremental trend in the west and north. Investigating a different issue within the area of Iran, Mohammadi & Sancholi (2013) found in their analysis of the precipitation concentration index variation in the semi-arid regions that the entire study area exhibited significant intra-annual variation, indicating the seasonal quality of precipitation in the arid regions of Iran. They also suggested that the increase in the seasonal rate and precipitation concentration in different parts has led to increased irregularity and fluctuation in the area.

In their analysis of precipitation over Saudi Arabia, Hasanean & Almazroui (2015) divided the statistical period into two periods. The first period showed slight fluctuation and an incremental trend from 1978 to 1993 (12.5 mm per decade), while the second period showed more significant precipitation fluctuation and a decreasing trend from 1993 to 2009 (35.1 mm per decade). These variations in precipitation played substantial roles in subtropical jet streams with two patterns: the Southern Oscillation Index and the North Atlantic Oscillation. In their analysis of the trends in heavy precipitation indices over Iran, Balling *et al.* (2016) analyzed trends in heavy precipitation indices over Iran and found an incremental trend across the country, with a significant trend observed from southwest to northeast. They also observed that this significant trend occurred particularly in the western and northern parts of Iran during the statistical period from 1950 to 2007, and the more significant occurrence in the cold seasons and the reduction in the others have caused the precipitation to concentrate over the country. Various regions worldwide have experienced this precipitation variation, such as China. Ma *et al.* (2015) found that precipitation intensity has changed over the past six decades, shifting from very low and mild to heavy and ultra-heavy. The frequency of floods and consecutive dry days has significantly increased, while the frequency of rainy days has decreased in most regions of China. Gallego *et al.* (2006) analyzed the variation in the frequency and intensity of daily precipitation over the Iberian Peninsula in Spain. According to the results, mean precipitation and the frequency of moderate to heavy precipitation have decreased during the past few decades, while the frequency of days with low to mild

precipitation has undergone an incremental trend. An entropy analysis was made by Mishra *et al.* (2009) based on the variation in precipitation over Texas, United States. It was found that the frequency of rainy days and precipitation have gradually decreased during the statistical period from 1900 to 2005, and precipitation entropy has increased over Texas as a consequence. The trends in pervasive and persistent drought over the entire state were incremental in the 1950s and from 1990 to 2006. Nazaripour & Mansouri Daneshvar (2014) investigated the spatial variation in 1-day precipitation in Iran. On that basis, precipitation in Iran had durations of 1–45 days, where 1-day precipitation has experienced a decreasing trend of 17.5% all over Iran. This has reduced mean precipitation and the total frequency of rainy days over a large part of the arid regions in the eastern and central half of the country, given the high frequency of such days concerning the total frequency of rainy days over that part of Iran. In a study of the variation in heavy and mean precipitation in Iran, Rahimi & Fatemi (2019) demonstrated that there has been a decreasing trend in annual precipitation during the period from 1960 to 2017 at most stations around the country. Heavy precipitation, rainy days, and severe wet periods have been restricted to the Caspian coasts in the north and the southern coasts. A review of research conducted both within Iran and the world reveals that most studies focus on variations in precipitation trends at different intensity levels. Therefore, this study aims to provide a more reliable and accurate assessment of the temporal entropy of precipitation and identify water resource regions in Iran by utilizing long-term, high spatial density versions of precipitation data.

2. DATA AND METHODS

2.1. Study area

The altitude conditions of the study area are shown in Figure 1(a), depicting two high-altitude regions over the country. One region is located along the northern coastline with an elevation of more than 5,000 m, while the other is situated between 30°N and 35°N on the central Zagros highlands in the western half of the country, with a height of more than 4,000 m. Iran's mean altitude is about 1,250 m, and low-altitude areas can be found along both the southern and northern coastlines as well as in the southwest. The central parts of the country are also considered leeward low-altitude areas. Figure 1(b) shows the long-term mean of the yearly precipitation rate from 1962 to 2019. As observed, the highest precipitation rate occurs along the southwestern coasts of the Caspian Sea. There is an average annual precipitation of over 1,500 mm over those areas. Along the Zagros Mountains in western Iran, between 28°N and 34°N and over the border of the west highlands, there is a precipitation rate exceeding 800 mm. However, in central parts of the country, average daily precipitation is minimized to only 56 mm. There are considerable differences in monthly and annual precipitation around Iran. Due to recent variability in precipitation-inducing weather systems across the country, attributed to global warming and climate change, researchers have noted clear variations in both precipitation and intensity. So, examining and scrutinizing the variability in spatial and temporal precipitation behavior is essential.

2.2. Data

The daily gridded precipitation data from the Asfazari database were utilized for this research. The database has been interpolated over Iran using the geostatistical method of Kriging. With a spatial resolution of $0.25° \times 0.25°$ (2,491 grids), this precipitation database was created in 20,819 days, from 01/01/1962 to 31/12/2019.

2.3. Methods

2.3.1. Entropy approach

The notion of entropy was first presented by Shannon (1948). The basics of maximum entropy were suggested by Jaynes later in 1957 (Jaynes 1957). Since then, the index has often been used in biological and hydrological science (Singh 1999). This index measures the distribution, uncertainty, irregularity and entropy, intensity variation, and precipitation amount (Kawachi *et al.* 2001). Entropy is a measure of the statistical distance between the actual monthly distribution of precipitation and the uniform distribution. It measures the temporal variability in monthly precipitation within a year, ranging between zero and Log2n bits. In this research, it was used to specify the spatiotemporal variability in monthly precipitation grid by grid over the study area. The index can be described as follows:

$$H = -\sum_{i=1}^{n} p_i \log_2 p_i \quad \text{(bit)} \tag{1}$$

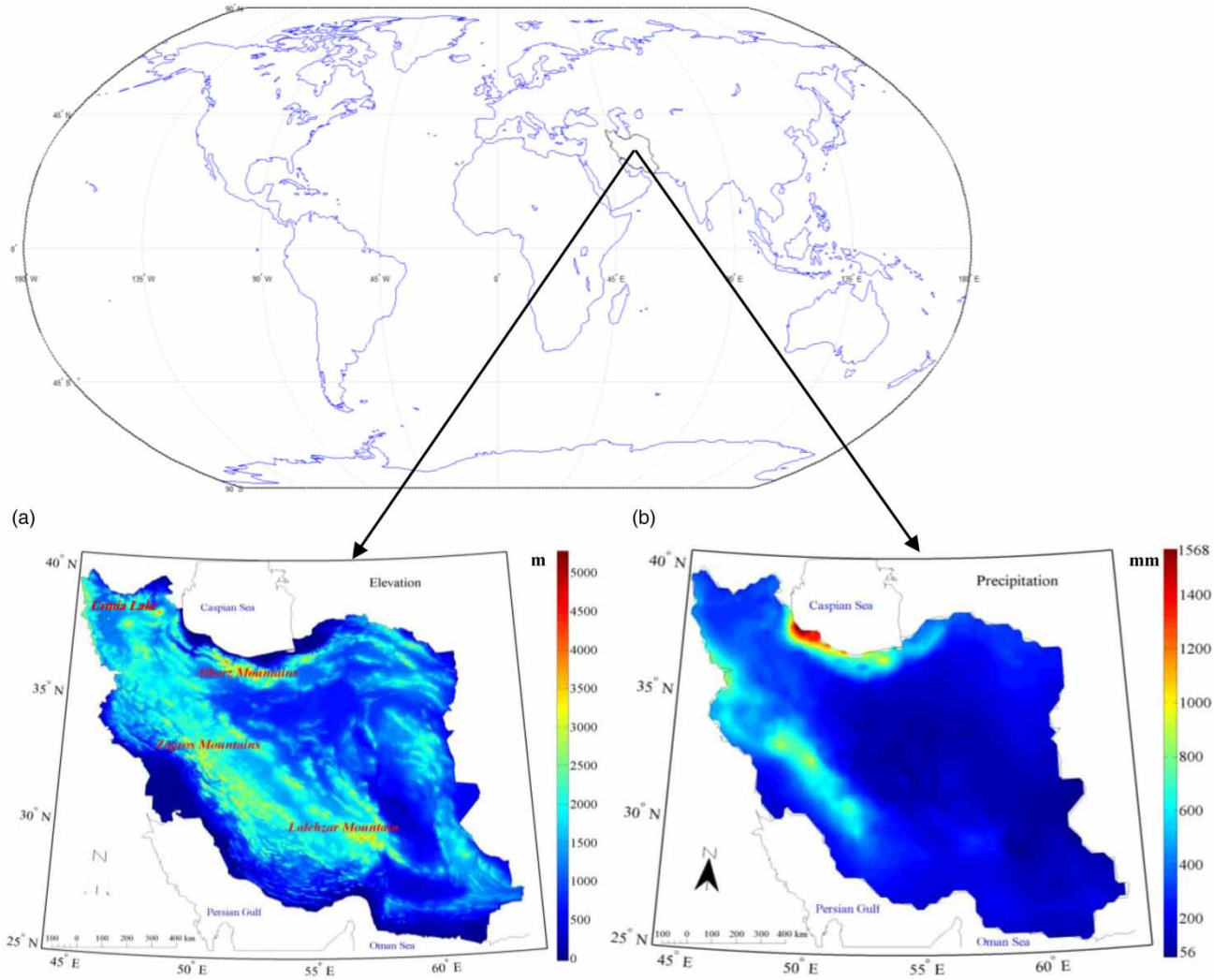

Figure 1 | Study area: (a) elevation in meters and (b) long-term mean of yearly precipitation rate in millimeters over Iran during the period from 1962 to 2019.

where 'bit' is used as the unit of measurement of the entropy H-Index and p_i is the relative frequency or probability of precipitation occurrence in the ith month. Equation (1) can be rewritten as follows:

$$H = -\sum_{i=1}^{n} \frac{r_i}{R} \log_2 \frac{r_i}{R} \quad \text{(bit)} \tag{2}$$

The probability of occurrence or the relative frequency of precipitation in each month of the year is obtained through the division of precipitation in that month r_i by total or annual precipitation R, and its distribution indicates the temporal distribution of precipitation in different months of the year. If the annual precipitation R occurs in only 1 month of the year, the value of the H-Index will be zero. Conversely, if precipitation is distributed evenly throughout the year, the H-Index will be maximized, amounting to Log2n. In other words, the larger the value of the H-Index, the more even the division of precipitation and the lower its temporal variability. The H-Index can be regarded as a scalar variable of precipitation variability. Given the time series corresponding to the monthly precipitation in n years at different grids, we can use the following

equation to estimate mean precipitation entropy.

$$\overline{H} = \frac{1}{n}\sum_{i=1}^{n} H_i \quad \text{(bit)} \tag{3}$$

2.3.2. Entropy-based variability

The *D*-Index indicates the difference between the highest probability of entropy and the entropy calculated from the analyzed time series, which is represented as the *D*-Index and can be calculated as follows:

$$D = \log_2 n - H \quad \text{(bit)} \tag{4}$$

where n is the length of the series period, and the *H*-Index is set to a value obtained by Equation (2). The larger the value of the *D*-Index, the greater the variability in precipitation. When yearly precipitation series for m years are available, the annual *D*-Index can be obtained using the following equation:

$$\overline{D} = \frac{1}{m}\sum_{i=1}^{m} D_i \quad \text{(bit)} \tag{5}$$

2.3.3. Trend

The nonparametric Mann–Kendall test was first presented by Mann (1945) and then extended by Kendall in 1948 (Kendall 1975). It can fit onto a non-normal time series that follows no particular distribution. This method is used to test the hypothesis that the sequence of data is random as opposed to the existence of a trend. In the current study, the modified nonparametric Mann–Kendall test was used to eliminate the impact of autocorrelation on trend detection (Hamed & Rao 1998). Sen's slope estimator was used to estimate the change rate. The World Meteorological Organization (WMO) has recommended two statistical methods, such as the Mann–Kendall test and Sen's slope estimator application.

2.3.4. Detection of water resource regions

Water resource regions are defined based on the coupled *H*-Index and annual precipitation over the study area, as follows:

Abundant and permanent: It consists of regions with mean annual precipitation values greater than the country's long-term mean precipitation and an insignificant seasonal pattern (the *H*-Index greater than the mean value over the country).

Deficient and permanent: It consists of regions with mean annual precipitation values less than the country's long-term mean precipitation and an insignificant seasonal pattern (the *H*-Index greater than the mean value over the country).

Deficient and concentrate: It consists of regions with mean annual precipitation values less than the country's long-term mean precipitation and a significant seasonal pattern (the *H*-Index less than the mean value over the country).

Abundant and concentrate: It consists of regions with mean annual precipitation values greater than the country's long-term mean precipitation and a significant seasonal pattern (the *H*-Index less than the mean value over the country).

All the statistical calculation and programming is done in the MATLAB environment.

3. RESULTS

3.1. Entropy index (*H*-Index) and disorder index (*D*-Index) over Iran

Figure 2 shows the spatiotemporal distribution of the precipitation *H*-Index and variability indices over Iran. According to Figure 2(a), the *H*-Index varies from 1.6 bits along the southern coastline to 3.4 bits along the northern coastlines. Moreover, the mean zonal rate of the *H*-Index over the country is 2.5. Following that along the Caspian coastline in the north, there is a high *H*-Index (2.6–3 bits) that stretches from the northwest to the southeast. This high *H*-Index is directed along the Zagros Mountains, starting from the northwestern corner and reaching areas in the southwest located at 30°N. This indicates that topography plays a role in increasing the frequency of rainy days in the region. In low-altitude areas such as the southwest, leeward areas in the Zagros Mountains, and the eastern and southern halves of the country, the *H*-Index gradually decreases. As the values of the *H*-Index decrease over the above areas, precipitation irregularity and frequency increase over time. In these areas, a major part of the annual precipitation occurs within 1 or 2 months of the year. In the northern half of the

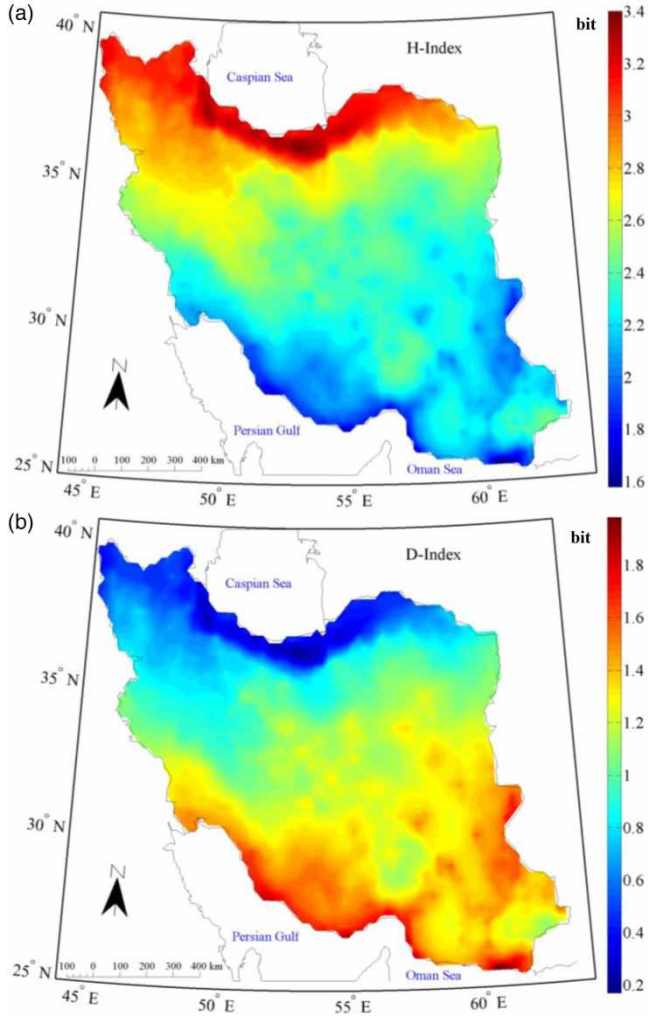

Figure 2 | (a): Mean *H*-Index and (b): *D*-Index over Iran during the period 1962–2019.

country; by contrast, precipitation distribution occurs over a longer period and in different months of the year. Conversely, the maximum value of precipitation variability is observed along the southern coastline as 1.8 bits, and the minimum value occurs along the northern coast as 0.2 bits (Figure 2(b)). The gradual rise in the precipitation variability index values toward the southern areas indicates an increase in irregularity and a decrease in the spatiotemporal consistency of precipitation. Investigating the spatial relationship between the *H*-Index and the *D*-Index over total grids (2,491 grids) with spatial parameters and precipitation is entirely the opposite. According to the *H*-Index, precipitation's consistency and temporal distribution decrease from the west to the east; in other words, precipitation becomes more centralized. A closer relationship is observed along the latitudes, where precipitation *H*-Index increases toward the north, indicating a greater and more regular precipitation per unit of time in northern areas. Additionally, areas with higher annual precipitation and more rainy days (the northern half) tend to have more regular and consistent precipitation. This shows a direct relationship between these factors and the *H*-Index (Table 1).

3.2. Variability and trend in the *H*-Index and the *D*-Index

In this step, the modified nonparametric Mann–Kendall test was fitted for the specification of the variability in the precipitation *H*-Index and *D*-Index over Iran during the analyzed period and the time series of the annual values of the above indices. According to Figure 3(a), there is a positive and significant trend in the *H*-Index in some northern areas, the shores of the north Oman Sea, and distributed areas in the center. Moreover, the maximum positive trend amounts to

Table 1 | Spatial correlation between the *H*-Index with spatial characteristics, precipitation, and rainy days

	Shorthand	*H*-Index	*D*-Index	*P*-value
Longitude	Lon	−0.498	0.498	0.001
Latitude	Lat	0.876	−0.875	0.001
Precipitation	P	0.536	−0.535	0.001
Rainy days[a]	RD	0.906	−0.905	0.001

[a]Number of days with precipitation amount of more than 0.1 mm.

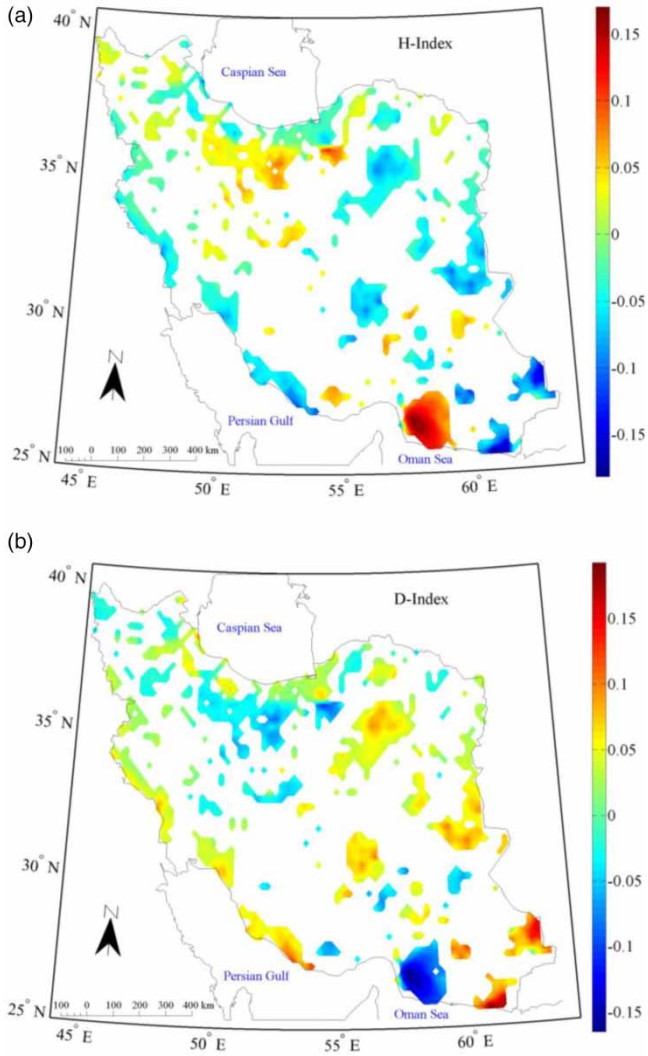

Figure 3 | (a): Trend and slope of the change rate of the *H*-Index and (b) the *D*-Index over Iran during the period of 1962–2019 at the level of 90% confidence.

more than 0.15 bits per decade over some regions, indicating an increase in the *H*-Index over time and an improvement in the regularity and consistency of precipitation. This suggests an increase in both the precipitation rate and frequency of rainy days in these areas. On the other hand, there is a negative and significant trend in the *H*-Index in eastern areas, along the western borderline, in the southwest and southeast, and along the Caspian coastline. These regions experience a decreased rate of *H*-Index per decade, with the greatest decrease observed for regions such as the southeastern corner and the northern

coastline of the Persian Gulf (−0.15). This indicates an increase in the irregularity of precipitation and a decrease in its consistency over time. However, when analyzing the precipitation *D*-Index (Figure 3(b)), it is observed that its trend rate values over Iran are inverse to those of the *H*-Index. Thus, the *D*-Index indicates negative and significant trends in areas such as the shores of the northern Oman Sea and northern Iran, which are located between 35°N and 37°N, where the *H*-Index shows positive and significant trends. This suggests that the concentration of precipitation decreases and its consistency increases over these regions during the examined statistical period. However, in areas including the western half and the east and southeast of the country, as well as other regions with negative trends in the *H*-Index, the precipitation *D*-Index exhibits positive trends. This indicates an increase in precipitation concentration, meaning a decrease in the distribution and frequency of rainy days over time.

Figure 4 displays the area-averaged annual time series of precipitation values, *H*-Index, *D*-Index, and frequency of rainy days. As can be observed, since 1998, the mean *H*-Index over Iran has gradually decreased along with a decrease in the mean frequency of rainy days and precipitation. This demonstrates a direct relationship with the *H*-Index. On the other hand, the precipitation *D*-Index behaves inversely to precipitation, *H*-Index, and the frequency of rainy days. The *D*-Index value over Iran has gradually increased since 1998 when sudden changes occurred in these analyzed parameters. The recent increase in the precipitation *D*-Index over Iran has been accompanied by a decrease in both precipitation and the frequency of rainy days. Additionally, there has been a decrease in consistency in precipitation as a consequence. Moreover, these examined indices are more closely related to the frequency of rainy days than to overall precipitation across the country. This shows that the uniformity and regularity of precipitation are more consistent with the parameters of rainy days.

3.3. Identification of water resource regions over Iran

Figure 5 shows the relationship between the indices of precipitation *H*-Index and *D*-Index and annual precipitation over Iran. According to Figure 5(a), the average annual precipitation in the country is 254.61 mm and the mean *H*-Index is 2.49 bits. Based on these values, Iran has been divided into four regions based on water resource conditions. Region I consists of regions with mean annual precipitation values greater than the long-term mean precipitation and the *H*-Index greater than the mean value over the country. This region, which covers 27.86% of the country's area, is characterized by abundant and consistent precipitation, with an average of 447 mm and an *H*-Index of 2.9. Region II comprises areas with annual precipitation values less than the mean value of Iran but the higher *H*-Index compared to the country's mean value. This region covers 14.17% of Iran's area and is classified as a region with deficient but permanent precipitation. The average precipitation in Region II is 176.63 mm, with a *H*-Index of 2.64. Region III is the largest water resource region in the country, covering 48.74% of Iran's area. It differs from the other regions in that both its mean zonal precipitation and *H*-Index rates are

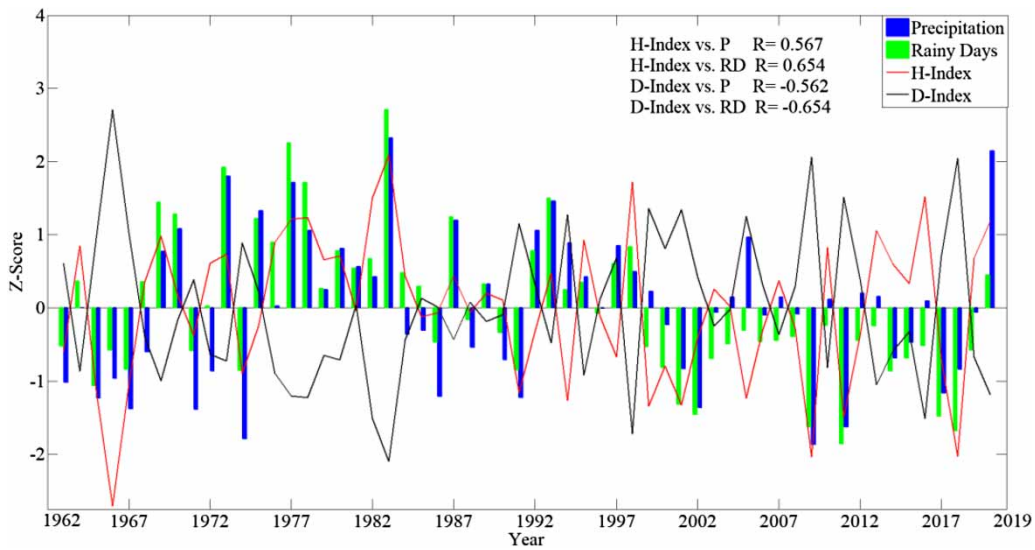

Figure 4 | Area-averaged of annual time series of precipitation *H*-Index, *D*-Index, frequency of rainy days, and received precipitation during the period 1962–2019. All correlations are significant at the level of 99% confidence.

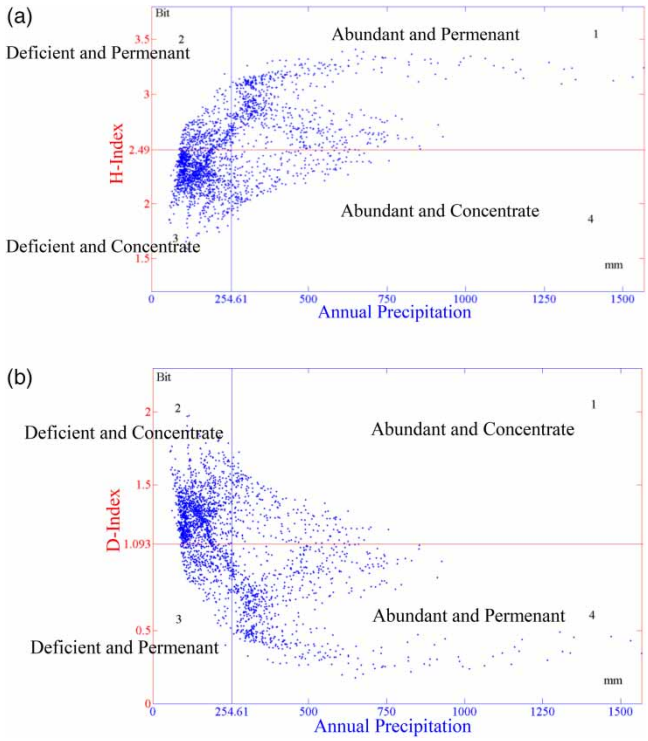

Figure 5 | (a): Relationship between precipitation *H*-Index and annual precipitation. (b) Relationship between *D*-Index and annual precipitation over Iran during the period 1962–2019.

lower than the country's long-term mean values. The mean precipitation over Region III is 141.76 mm, and the *H*-Index is 2.25. Based on this, this region is known for deficient and concentrate precipitation occurring within an extremely short period in winter each year. Region IV, which covers 9.23% of the area, is the least extensive water resource region in Iran. It exhibits an average zonal precipitation of 389.36 mm, which is greater than the mean long-term precipitation over the country. The *H*-Index for this region is 2.24, which is less than the mean value of Iran. Therefore, this water resource region, composed of regions located in the southwest, is considered to have abundant but concentrate precipitation. In other words, there is plentiful precipitation in the region, but it occurs in a concentrated and inconsistent manner within a short period of each year. The analysis of the precipitation *D*-Index in Figure 5(b) involves specifying four water resource regions, similar to the *H*-Index. The mean value of the *D*-Index over the country is 1.093, behaving inversely with the *H*-Index. The exact boundaries between the water resource regions are specified in terms of both indices.

3.4. Water resource regions

For the specification of variability over the four water resource regions in Iran, in terms of the values of the *H*-Index and annual precipitation, the boundaries between them were calculated and interpreted for three periods: the overall period from 1962 to 2019, the period before the sudden change (1962–1998), and the period after that (1999–2019) (Figure 6).

3.4.1. Abundant and permanent

According to Figure 6(a), during the statistical period of 57 years, the abundant and permanent water resource region in Iran was located in the northern half of the country along the Zagros Mountains in the west and Alborz Mountains in the north.

3.4.2. Deficient and permanent

The water resource region with deficient and permanent precipitation is found in the southern part of the Alborz Mountains and the eastern part of the Central Zagros Mountains, extending longitudinally up to the northeastern borders.

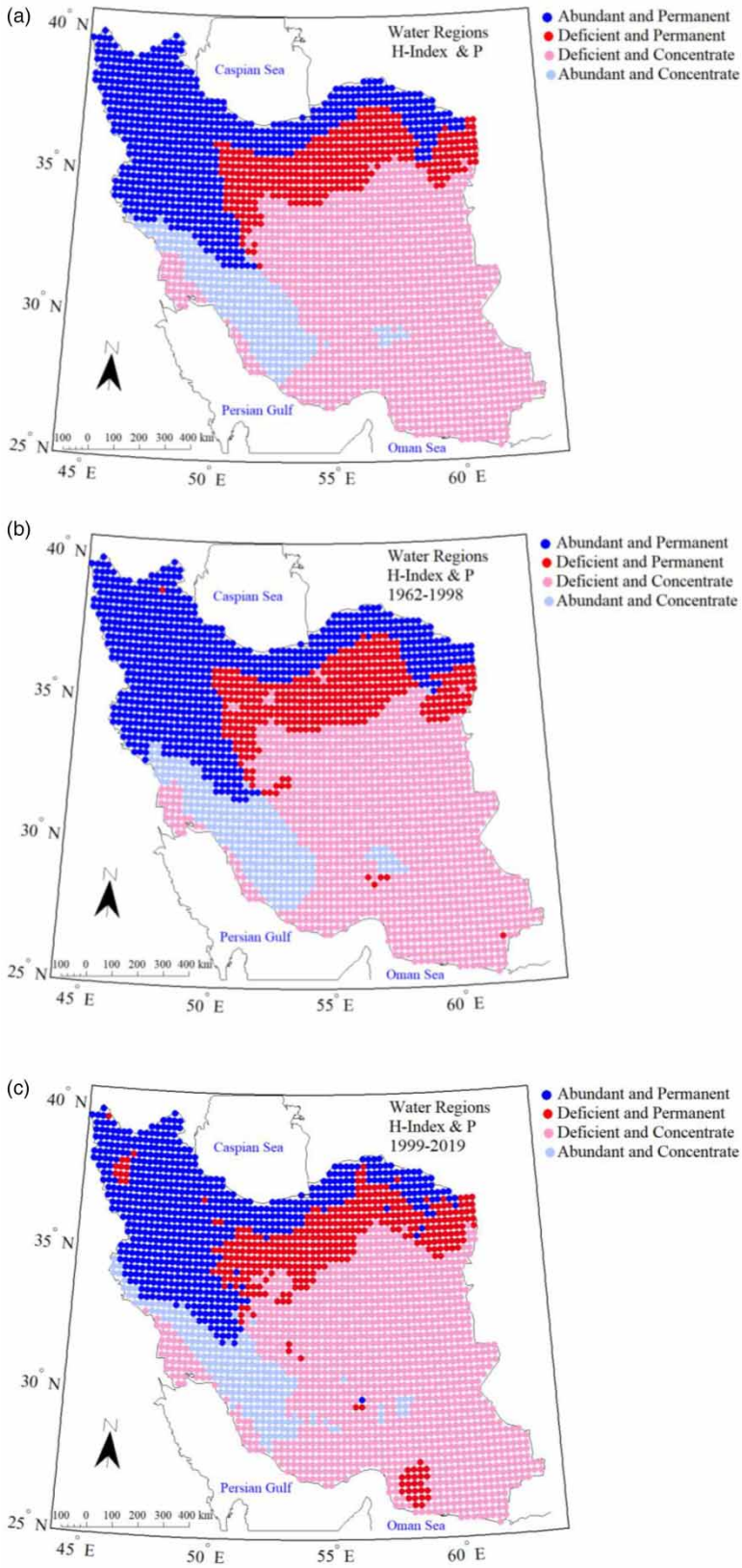

Figure 6 | Variations in the range of water areas of the country: (a) in the statistical period of 1962– 2019, (b) period before the mutation (1962–1998), (c) after it (1999–2019) based on the *H*-Index and annual precipitation.

3.4.3. Deficient and concentrate

The country's most extensive water resource region has experienced deficient and concentrate precipitation, covering large parts of the south, center, and east.

3.4.4. Abundant and concentrate

Finally, the least vast water resource region is located in southwest Iran and consists of the southern part of the Zagros Mountains.

The considerable sudden change observed in 1998 in the values of the *H*-Index and precipitation parameters caused the long-term period under examination to be divided into two periods: one before that year's sudden change and the other after that. This division allowed for a comparison of the variability in water resource regions between the two periods. The comparison of areas before and after the sudden change (Figure 6(b) and 6(c)) indicates a significant difference in their sizes. The permanent water resource regions with abundant and deficient precipitation and also abundant and concentrate regions experienced a reduction after 1998. In contrast, the region with deficient and concentrate precipitation has extended over a larger region from 46.01% to more than 50.54% of Iran's total area. The most severe reduction was observed in the abundant and permanent water resource region, with a decrease of 2.97% (equivalent to 48,957.04 km^2) in the country's northern half (Table 2). It is worth noting that regions with deficient and permanent precipitation emerged during the second period (1999–2019) within this region around Lake Urmia in the northwest, as well as at various points in the north and northeast. The lowest variability has also occurred in the water resource region with deficient and permanent precipitation, with a decrease of −0.12%. The region with deficient and concentrate precipitation has extended toward the north, also involving the northern part of Khuzestan Province in the southwest, the center, and the northeastern borders. The only region that has shifted from a region with deficient and concentrate precipitation to one with deficient and permanent precipitation is located on the shores north of the Oman Sea and east of the Strait of Hormuz. This indicates a greater distribution of rainy days per unit of time over the year in the region, which calls for further investigation to address emerging questions. The shift in water resource distribution can be attributed to a decrease in precipitation concentration and an increase in temporal consistency of rainy days along the northern coasts of the Oman Sea. This is due, in turn, to the rising sea temperatures (Khan *et al.* 2004; Pionkovski & Chiffings 2014; Bahri & Khosravi 2020), increased specific humidity along the southern coasts of Iran in recent years (Dehghani *et al.* 2018; Darand *et al.* 2019), consistent with an increase in fall precipitation along the southeastern coasts of the country (Mosaffa *et al.* 2020), integrated moisture flux convergence from the Oman Sea and Arabian Sea, as well as other relevant trends. The area of abundant and concentrate water resources has also decreased during this second period, mainly in the southern part of the Zagros Mountains in the south of 30°N, and in the highlands of Lalehzar in Kerman Province at 57°E. Despite a decrease of 1.44% in its area, it has expanded toward northern latitudes to cover parts of Iran's western border between 34°N and 35°N.

Figure 7 shows the variability in the extension of Iran's water resource regions during the long period and the short divisions in terms of the precipitation *D*-Index. As can be observed, the spatial distribution of the areas (Figure 7(a)) is the same as that in Figure 6 for the *H*-Index but different in terms of the values of the two indices. In terms of the *D*-Index, only the water resource region with deficient and concentrate precipitation becomes more extensive during the second period, i.e., after the sudden change (Figure 7(c)), particularly in central parts of Iran and in the southwest. This indicates an increase in precipitation concentration and consistency in this part of the country, while other water resource regions have become less extensive. The severest decrease has occurred at a rate of about 3%, equivalent to 50,941 km^2, for the

Table 2 | Variations of the country's water regions in the two periods before the mutation (1962–1998) and after it (1999–2019) based on the *H*-Index

	Area (%)			
Category	**Period 1998–1962**	**Period 1999–2019**	**Area variation (%)**	**Extent variation (km^2)**
Abundant and permanent	29.06	26.09	−2.97	−48,957.04
Deficient and permanent	15.05	14.93	−0.12	−1,984.74
Deficient and concentrate	46.01	50.54	4.53	74,758.73
Abundant and concentrate	9.87	8.43	−1.44	−23,816.94

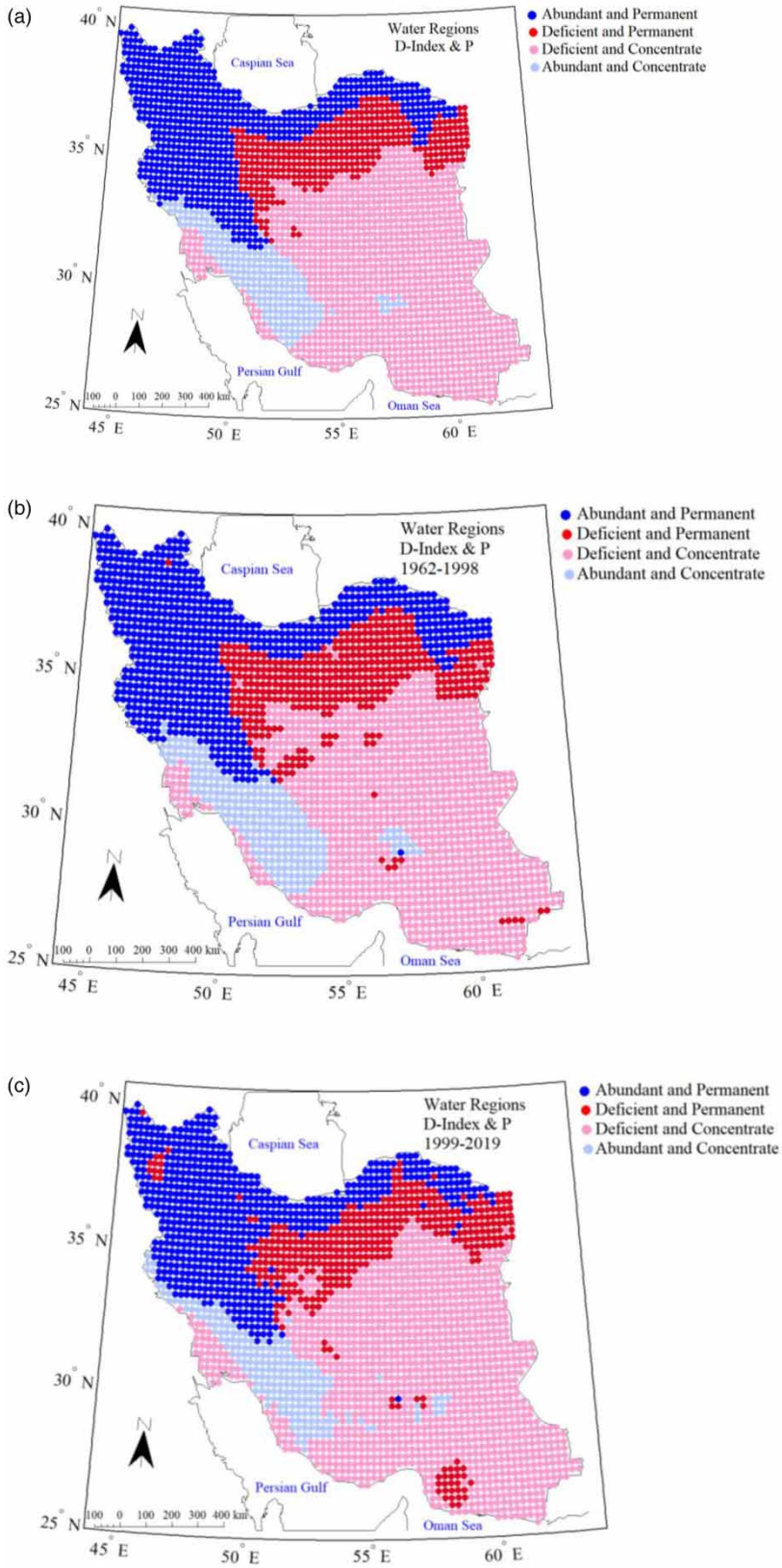

Figure 7 | Variations in the range of water regions of the country: (a) in the statistical period of 1962–2019, (b) period before the mutation (1962–1998), and (c) after it (1999–2019) based on the variation index and annual precipitation.

Table 3 | Variations of the country's water areas in the two periods before the mutation (1962–1998) and after it (1999–2019) based on the *D*-Index

Category	Area (%)		Area variation (%)	Extent variation (km^2)
	Period 1962–1998	Period 1999–2019		
Abundant and permanent	29.43	26.33	−3.09	−50,941.79
Deficient and permanent	17.06	16.30	−0.76	−12,570.05
Deficient and concentrate	44.00	49.17	5.18	85,344.04
Abundant and concentrate	9.51	8.19	−1.32	−21,832.20

abundant and concentrate region located in the southern part of the Zagros Mountains in the southwest. This region has shifted to an area with deficient and permanent precipitation. Furthermore, the most extensive region has been the one with deficient and permanent precipitation, while the least extensive region has been the one with abundant and permanent precipitation (Table 3).

4. DISCUSSION

The analysis of maps displaying the trends in the *H*-Index and its variability demonstrates that the variability in their values is distributed all over the country unlike what has been observed on the maps for the mean. Thus, the range of the significant negative trend is greater than that of the positive trend based on the *H*-Index. Moreover, the maximum significant negative trend is observed with a decreasing rate of 0.15 bits per decade at the southeastern corner in the east and north of the Persian Gulf coasts. In contrast, the maximum positive trend is observed with the same intensity to the north of the Oman Sea coasts and along the Alborz Mountains in the north. The trend in the *D*-Index is exactly inverse to that in the *H*-Index, indicating an increase in the consistency and reliability of precipitation occurrence for regions with positive trends in the *H*-Index. Conversely, there is a decrease in temporal distribution and an increase in precipitation concentration for regions with negative trends. Given a significant sudden change in the frequency of rainy days and *H*-Index values in 1998, we divided the long-term period (1962–2019) into two periods: before and after 1998. We compared the precipitation index and parameter values between these two periods. It was found that after 1998, values of the *H*-Index, the frequency of rainy days, and mean precipitation have decreased, while the *D*-Index value has increased. These results are consistent with an incremental trend in severe and pervasive droughts in Iran in recent years (Keshavarz *et al.* 2012; Hosseini *et al.* 2021).

In the following step, Iran was divided into four regions based on water resources, taking into account the values of the *H*-Index and the *D*-Index as well as annual precipitation. These regions were categorized as follows: abundant and permanent, deficient and permanent, deficient and concentrate, and abundant and concentrate. Comparing and analyzing these water resource regions in terms of the *H*-Index before and after 1998 revealed significant changes during the second period (1999–2019). The regions with abundant and permanent, deficient and permanent, and abundant and concentrate precipitation became less extensive, while the regions with deficient and concentrate precipitation expanded toward northern latitudes as well as areas in the center, northeast, and southwest. The most significant reduction occurred in the abundant and permanent water resource region, with a decrease of 2.97% in the country's northern half. It is crucial to note that parts of the abundant and permanent region in the northwestern corner, along with other scattered areas in the northern half of the country, shifted to the region with deficient and permanent precipitation. This shift could have negative consequences on the hydrologic cycle and available water resources in those regions. To meet preeminent water needs, careful and early water management strategies must be implemented to reduce water waste and store excess water during the rainy season (Mishra *et al.* 2009). According to Fathian *et al.* (2020), there has been a decreasing trend in precipitation and its intensity and also an incremental trend in the frequency of consecutive days without precipitation in recent years over the western, northern, and northwestern parts of Iran. HadiPour *et al.* (2020) addressed the decreasing trend in precipitation over more than 11% of the north half of the country, as well as a decrease of 14 mm per decade over semi-arid regions in the northwest during the past decade.

Furthermore, in the western part of the Alborz Mountains at 35°N and 50°E, there has been a shift from a region with deficient and permanent precipitation to an abundant and permanent region during the second period. In contrast, regions

to the north of the Oman Sea coasts have shifted from an abundant and concentrate region to one with deficient and permanent precipitation. These shifts indicate a decrease in precipitation concentration and an increase in the temporal distribution of rainy days throughout the year. The spatial distribution of the water resource regions identified by the *D*-Index was the same as that for the *H*-Index, differing only in the variability in the extension of the areas. Thus, it was only the region with deficient and permanent precipitation that became more extensive during the second period in terms of the precipitation *D*-Index, while the abundant and concentrate region experienced the highest decrease in extension, with a rate of −3.09%. In conclusion, it can be stated that variability has increased in Iran's water resource regions, particularly in arid and low-precipitation areas, moving toward the northern half and reducing the extension of high-precipitation humid areas. These changes are characterized by an increase in deficient and concentrate regions and a decrease in abundant and permanent precipitation regions. These changes in climatic elements, including temperature, can mainly be attributed to negative human activities and climate change, resulting in significant decreases in water resource conditions and precipitation patterns worldwide (Westra *et al.* 2013; Grill *et al.* 2015). Another important consequence of regional warming and Iran's climate change, especially in recent decades, is an upward trend in temporal precipitation concentration and an increase in the frequency of extremely rainy days (Vaghefi *et al.* 2019; Tegegne *et al.* 2021).

5. CONCLUSIONS

The current study aimed to identify the spatiotemporal variability in monthly precipitation and specify the water resource regions over Iran by applying the entropy method (*H*-Index) and its variability (*D*-Index). To do this, daily precipitation data from 01/01/1962 to 31/12/2019 with a spatial resolution of $0.25° \times 0.25°$ were used. The following conclusions are drawn from this study:

(1) The entropy value (*H*-Index) is varied over Iran from 1.6 bits in the southern coasts, southwest, and eastern half of the country to 3.4 bits along the Caspian coasts, and the western half along the Zagros Mountains.
(2) The analysis of the spatial correlation demonstrated a direct relationship over Iran between latitude, precipitation, and the frequency of rainy days on one hand, and the *H*-Index on the other. This relationship was inversely related to longitude.
(3) It was found that after 1998, values of the *H*-Index, the frequency of rainy days, and mean precipitation have decreased, while the *D*-Index value has increased.
(4) Coupling of the values of the *H*-Index and *D*-Index with annual precipitation enables detection of the potential availability of water resources. Based on these values, Iran was divided into four distinct regions: abundant and permanent, deficient and permanent, deficient and concentrate, and abundant and concentrate.
(5) Comparing the *H*-Index value before and after 1998 revealed significant changes over water resource regions during the second period (1999–2019). The regions with abundant and permanent, deficient and permanent, and abundant and concentrate precipitation became less extensive, while the regions with deficient and concentrate precipitation expanded toward northern latitudes as well as areas in the center, northeast, and southwest. It is crucial to note that parts of the abundant and permanent region in the northwestern corner, along with other scattered areas in the northern half of the country, shifted to the region with deficient and permanent precipitation.

ACKNOWLEDGEMENTS

We extend our sincere gratitude to Professor Seyed Abolfazl Masoodian for providing daily gridded precipitation data from the Asfazari database.

AUTHORS CONTRIBUTIONS

M.D. studied and worked on conceptualization and methodology, wrote the original draft, and reviewed and edited the manuscript. F.P. worked on formal analysis, data collection, conceptualization, and analysis. All authors read and approved the final manuscript.

FUNDING

This work is based upon research funded by the Vice Chancellorship of Research and Technology, University of Kurdistan.

DATA AVAILABILITY STATEMENT

Data cannot be made publicly available; readers should contact the corresponding author for details.

CONFLICT OF INTEREST

The authors declare there is no conflict.

REFERENCES

Bahri, A. & Khosravi, Y. 2020 Investigation of long term trend of spatio-temporal changes of sea surface temperature in Oman Sea. *J. Appl. Res. Geogr. Sci.* **58**, 199–217.

Balling, R., Keikhosravi-Kiany, M. S., Sen Roy, S. & Khoshhal, J. 2016 Trends in extreme precipitation indices in Iran: 1951–2007. *Adv. Meteorol.* **2016**, 1–8. http://dx.doi.org/10.1155/2016/2456809.

Darand, M., Pazhooh, F. & Saligheh, M. 2019 Trend analysis of tropospheric specific humidity over Iran during 1979–2016. *Int. J. Climatol.* **39** (10), 4058–4071. https://doi.org/10.1002/joc.6059.

Dehghani, T., Salighe, M. & Alijani, B. 2018 The effect of climate change on the distribution of specific moisture in the northern coasts of the Persian Gulf. *Nat. Geogr.* **11** (39), 33–46.

Fathian, F., Ghadami, M., Haghighi, P., Amini, M., Naderi, S. & Ghaedi, Z. 2020 Assessment of changes in climate extremes of temperature and precipitation over Iran. *Theor. Appl. Climatol.* **141**, 1119–1133. https://doi.org/10.1007/s00704-020-03269-2.

Gallego, M. C., Garc, J. A., Vaquero, J. M. & Mateos, V. L. 2006 Changes in frequency and intensity of daily precipitation over the Iberian Peninsula. *J. Geophys. Res.* **111** (D24), 1–15. https://doi.org/10.1029/2006JD007280.

Grill, G., Lehner, B., Lumsdon, A. E., MacDonald, G. K., Zarfl, C. & Liermann, C. R. 2015 An index-based framework for assessing patterns and trends in river fragmentation and flow regulation by global dams at multiple scales. *Environ. Res. Lett.* **10** (1), 1–15. https://doi.org/10.1088/1748-9326/10/1/015001.

HadiPour, S., Wahab, A. K. A. & Shahid, S. 2020 Spatiotemporal changes in precipitation indicators related to bioclimate in Iran. *Theor. Appl. Climatol.* **141**, 99–115. https://doi.org/10.1007/s00704-020-03192-6.

Hamed, K. H. & Rao, A. R. 1998 A modified Mann–Kendall trend test for autocorrelated data. *J. Hydrol.* **204**, 182–196.

Hasanean, H. & Almazroui, M. 2015 Rainfall: Features and variations over Saudi Arabia: a review. *Climate* **3** (3), 578–626. https://doi.org/10.3390/cli3030578.

Hosseini, A., Ghavidel, Y., Khorshiddoust, A. M. & Farajzadeh, M. 2021 Spatio-temporal analysis of dry and wet periods in Iran by using global precipitation climatology center-drought index (GPCC-DI). *Theor. Appl. Climatol.* **143**, 1035–1045. https://doi.org/10.1007/s00704-020-03463-2.

Javari, M. 2016 Trend and homogeneity analysis of precipitation in Iran. *Climate* **4** (3), 44. https://doi.org/10.3390/cli4030044.

Jaynes, E. T. 1957 Information theory and statistical mechanics. *Phys. Rev.* **106**, 620–630. https://doi.org/10.1103/PhysRev.106.620.

Kawachi, T., Maruyama, T. & Singh, V. P. 2001 Rainfall entropy for delineation of water resources regions in Japan. *J. Hydrol.* **246** (1–4), 36–44. https://doi.org/10.1016/S0022-1694(01)00355-9.

Kendall, M. G. 1975 *Rank Correlation Methods*. Griffin, London.

Keshavarz, M. R., Vazifedoust, M., Fatahi, E. & Behyar, M. B. 2012 Distribution pattern of direction and intensity of drought changes in Iran using Palmer drought intensity distribution index. *J. Appl. Res. Geogr. Sci.* **27**, 98–101.

Khan, T. M. A., Quadir, D. A., Murty, T. S. & Sarker, M. A. 2004 Seasonal and interannual sea surface temperature variability in the coastal cities of Arabian Sea and Bay of Bengal. *Nat. Hazards* **31**, 549–560. https://doi.org/10.1023/B:NHAZ.0000023367.66009.1d.

Ma, S., Zhou, T., Dai, A. & Han, Z. 2015 Observed changes in the distributions of daily precipitation frequency and amount over China from 1960 to 2013. *J. Clim.* **28**, 6960–6979. https://doi.org/10.1175/JCLI-D-15-0011.1.

Mann, H. B. 1945 Nonparametric tests against trend. *Econom. J. Econom. Soc.* **13**, 245–259.

Marengo, J., Liebmann, B., Kousky, V. E., Filizola, N. & Wainer, I. 2001 On the onset and end of the rainy season in the Brazilian Amazon Basin. *J. Clim.* **14**, 833–852. https://doi.org/10.1175/1520-0442(2001)014 < 0833:OAEOTR > 2.0.CO;2.

Masoudian, S. A. 2006 Demarcation of Iran's water areas with the help of precipitation turbulence index. *J. Isfahan Univ.* **20** (1), 1–14. Available from: https://www.magiran.com/paper/409729.

Masoudian, S. A. 2011 *Climate of Iran*. Sharia Toos, Esfahan.

Mishra, A. K., Özger, M. & Singh, V. P. 2009 An entropy-based investigation into the variability of precipitation. *J. Hydrol.* **370**, 139–154. https://doi.org/10.1016/j.jhydrol.2009.03.006.

Mohammadi, M. & Sancholi, M. 2013 Investigation of rainfall concentration index changes in semi-arid regions of Iran. In: *National Conference on Natural Resources Management*, 27 Feb 2014, Golestan Province. Gonbad Kavous University.

Mosaffa, H., Sadeghi, M., Hayatbini, N., Afzali Gorooh, V., Akbari Asanjan, A., Nguyen, P. & Sorooshian, S. 2020 Spatiotemporal variations of precipitation over Iran using the high-resolution and nearly four decades satellite-based PERSIANN-CDR dataset. *Rem. Sens.* **12** (10), 1584. https://doi.org/10.3390/rs12101584.

Nazaripour, H. & Mansouri Daneshvar, M. R. 2014 Spatial contribution of one-day precipitations variability to rainy days and rainfall amounts in Iran. *Int. J. Environ. Sci. Technol.* **11**, 1751–1758. https://doi.org/10.1007/s13762-014-0616-x.

Pionkovski, S. A. & Chiffings, T. 2014 Long-term changes of temperature in the Sea of Oman and the Western Arabian sea. *Int. J. Oceans Oceanogr.* **8**, 53–72.

Rahimi, M. & Fatemi, S. S. 2019 Mean versus extreme precipitation trends in Iran over the period 1960–2017. *Pure Appl. Geophys.* **176**, 3717–3735. https://doi.org/10.1007/s00024-019-02165-9.

Roushangar, K. & Alizadeh, F. 2018 Entropy-based analysis and regionalization of annual precipitation variation in Iran during 1960–2010 using ensemble empirical mode decomposition. *J. Hydroinform.* **20** (2), 468–485. https://doi.org/10.2166/hydro.2018.037.

Shannon, C. E. 1948 A mathematical theory of communication. *Bell Syst. Tech. J.* **27** (3), 379–423. https://doi.org/10.1002/j.1538-7305.1948.tb01338.x.

Silva, V. D. P. R. D., Belo, F. A. F., Singh, V. P., Almeida, R. S. R., Silva, B. B. D., de Sousa, I. F. & Holanda, R. M. D. 2017 Entropy theory for analyzing water resources in northeastern region of Brazil. *Hydrol. Sci. J.* **62** (7), 1029–1038. https://doi.org/10.1080/02626667.2015.1099789.

Singh, V. P. 1999 The use of entropy in hydrology and water resources. *Hydrol. Process.* **11** (6), 587–626. https://doi.org/10.1002/(SICI)1099-1085(199705)11:6<587::AID-HYP479 > 3.0.CO;2-P.

Tegart, W. J., Mc, G., Sheldon, G. W. & Griffths, D. C. 1990 *Climate Change: The IPPC Scientific Assessment*. Australian Government Publishing Service, Canberra.

Tegegne, G., Melesse, A. M. & Alamirew, T. 2021 Projected changes in extreme precipitation indices from CORDEX simulations over Ethiopia, East Africa. *Atmos. Res.* **247**, 105156. https://doi.org/10.1016/j.atmosres.2020.105156.

Vaghefi, S. A., Keykhai, M., Jahanbakhshi, F., Sheikholeslami, J., Ahmadi, A., Yang, H. & Abbaspour, K. C. 2019 The future of extreme climate in Iran. *Sci. Rep.* **9**, 1464. https://doi.org/10.1038/s41598-018-38071-8.

Westra, S., Alexander, L. V. & Zwiers, F. W. 2013 Global increasing trends in annual maximum daily precipitation. *J. Clim.* **26** (11), 3904–3918. https://doi.org/10.1175/JCLI-D-12-00502.1.

Zamani, R., Mirabbasi, R., Nazeri, M., Meshram, S. G. & Ahmadi, F. 2018 Spatio-temporal analysis of daily, seasonal and annual precipitation concentration in Jharkhand state, India. *Stoch. Environ. Res. Risk Assess.* **32**, 1085–1097. https://doi.org/10.1007/s00477-017-1447-3.

First received 1 August 2023; accepted in revised form 26 February 2024. Available online 9 March 2024